

Bloch-surface-wave-induced Fano resonance in magnetophotonic crystals

M. N. Romodina,¹ I. V. Soboleva,^{1,*} A. I. Musorin,¹ Y. Nakamura,² M. Inoue,² and A. A. Fedyanin^{1,†}

¹Faculty of Physics, Lomonosov Moscow State University, Moscow 119991, Russia

²Toyohashi University of Technology, Toyohashi 441-8580, Japan

(Received 8 January 2017; revised manuscript received 27 June 2017; published 1 August 2017)

We have observed the Fano-type Faraday rotation spectrum in a one-dimensional magnetophotonic crystal at the Bloch surface wave (BSW) resonance and found that it is a result of the coupling between the *s*-polarized BSW and the *p*-polarized waveguiding modes of the magnetophotonic crystal. The shape of the resonance is determined by the relative position and spectral splitting of the modes.

DOI: [10.1103/PhysRevB.96.081401](https://doi.org/10.1103/PhysRevB.96.081401)

Magneto-optical phenomena, such as Faraday and Kerr effects, are the fingerprints of the spin-orbital interaction that appears when light couples with a magnetized medium and can be significantly increased near spectrally narrow optical resonances [1–5]. Magnetophotonic crystals (MPCs) [6] that have resonances in the photonic density of states at the band-gap edge provide extensive opportunities for controlling the Faraday and Kerr effects. Under an external magnetic field applied to an MPC, an increase in the Faraday effect is observed at the photonic-band-gap edge [7–9] due to the slow light effect [10]. A stronger enhancement of the Faraday rotation angle can be obtained at the narrow resonances of MPC reflectance spectra related to the multipass traveling of light in the MPC microcavity spacer [11–14]. It is caused by the splitting of the resonance for the right and left circularly polarized waves in the medium under the magnetic field [15]. Since the wave phase is changing by π upon tuning through the resonance, the polarization plane rotation of the outgoing wave can reach up to $\pi/2$ if the spectral distance between split resonances is sufficiently large. Thus, in the presence of narrow optical resonances, the Faraday rotation angle is determined both by the magnetic properties of the material affecting the splitting and by the Q factor of the resonances, which define their spectral width [6].

However, besides the Faraday rotation enhancement, the magneto-optical control of light implies different directions of polarization plane rotation, linear-to-circular and other polarization transformations. These opportunities can be opened by the use of polarization-sensitive MPCs that have resonances only for specific linear polarizations of the incident light. An example is a 1D-MPC with a specially selected top layer thickness that supports the Bloch surface electromagnetic wave (BSW) excitation [16–19]. The proper choice of the MPC parameters provides the means to observe the *s*-polarized BSW and *p*-polarized waveguiding mode (WGM) of the MPC in the same spectral region [20]. Recently, we have theoretically studied the optimal conditions for BSW excitation in magnetophotonic crystals [21]. The BSW excitation in MPCs was shown to cause the Faraday rotation of the light polarization inside the structure (Fig. 1). *P*-polarized light appears due to Faraday rotation and excites the WGM. The interplay of the

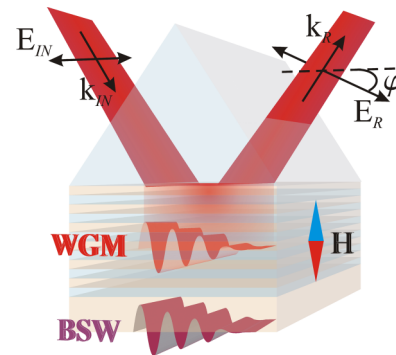


FIG. 1. Schematic representation of the experiment.

BSW and WGM results in an enhancement of the Faraday rotation angle φ between the directions of the incident and reflected electric vectors E_{IN} and E_R . The lineshape of the Faraday rotation spectra becomes Fano shaped. Here, we experimentally demonstrate how a fundamental property of magneto-optical effects to couple two linearly polarized modes allows one to control and modify the values of Faraday rotation angles. The spectral lineshape of the Faraday rotation is shown to be Fano shaped and is determined by the relative positions of the BSW and WGM resonances.

The chosen magnetophotonic crystal sample consists of 15 alternating layers of fused quartz and Bi-substituted yttrium-iron-garnet (Bi:YIG) ($n_q = 1.45$ and $n_{YIG} = 2.15$ at a wavelength of 700 nm) on a gadolinium gallium garnet (sGGG) substrate. The photonic band gap at normal incidence of light is supposed to be centered at $\lambda_0 = 830$ nm. The top layer thickness is 390 nm, and the other layers have a thickness of $\lambda_0/4$. Figure 2 shows the reflectance of the magnetophotonic crystal depending on the wavelength and the angle of incidence calculated using the transfer matrix technique [22,23]. When the sample is illuminated by *s*-polarized light behind the light line, the BSW appears inside the photonic band gap. If the incident light is *p* polarized, the WGM shown in Fig. 2 as red curves is excited in the same spectral range. The distributions of the electromagnetic field amplitudes in the MPC layers calculated for these two modes are shown in the bottom panels of Fig. 2. At the BSW mode, the electromagnetic field is concentrated at the photonic crystal/air interface and exponentially decreases deep into the MPC. The WGM profile has an envelope increasing to the photonic crystal center, which is typical for waveguiding modes.

* Also at: Frumkin Institute of Physical Chemistry and Electrochemistry, Russian Academy of Sciences, Moscow 119071, Russia.

† fedyanin@nanolab.phys.msu.ru

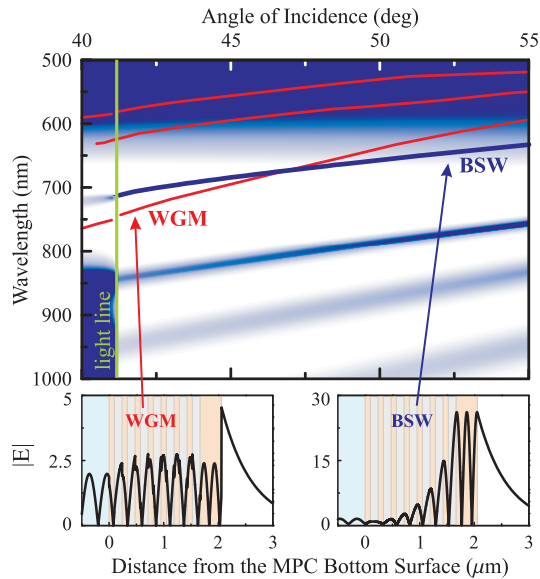


FIG. 2. Top panel: Magnetophotonic crystal reflectance depending on the wavelength and the angle of incidence of the s -polarized light. The blue curves are the BSW and s -polarized waveguiding modes, and the red curves mark the dispersion curves of dark p -polarized waveguiding modes. Bottom panel: Distributions of the electric field amplitude across the magnetic (yellow) and nonmagnetic (gray) layers of magnetophotonic crystal at the WGM and BSW. The amplitude of the electric field in front (in the substrate, blue) and behind (in the air, white) the sample is also shown.

The magnetophotonic crystal sample was fabricated by ion-beam sputtering of Bi:YIG and SiO₂ targets onto an sGGG substrate. Each bilayer was annealed for 15 minutes at a temperature of 750 °C. Transmittance spectra and spectra of the Faraday rotation angle of the incident light passing through the MPC sample were measured simultaneously. The experimental setup is schematically shown in Fig. 3(b). The sample was illuminated by a white-light beam of a filament lamp L passed through a collimator and a polarizer P . The magnet M was located face to face with the back side of the sample, producing a magnetic field with a strength of 1 kOe. This setup provides the possibility of both transmittance and reflectance spectroscopy via changing the angle of incidence θ and detection angle. Light passing through or reflected from the sample passed through an analyzer A and was detected by the spectrometer S . Spectra of the Faraday rotation angle were determined from the phase difference of Malus's law measured for opposite directions of the magnetic field [24]. The magnetic properties of the sample were characterized using the vibrating sample magnetometer technique [Fig. 3(c)]. The dependence of the sample magnetization on the strength of the applied external magnetic field demonstrates the hysteresis caused by the ferrimagnetic Bi:YIG layers and shows that the external field strength of 1 kOe is sufficient for saturating the magnetization curve. Figure 3(a) shows the experimental and calculated transmittance spectra of the magnetophotonic crystal sample and the corresponding Faraday rotation spectra. On the right edge of the photonic band gap, there is a slight increase in the Faraday rotation, which was previously observed in similar structures due to multipass traveling of

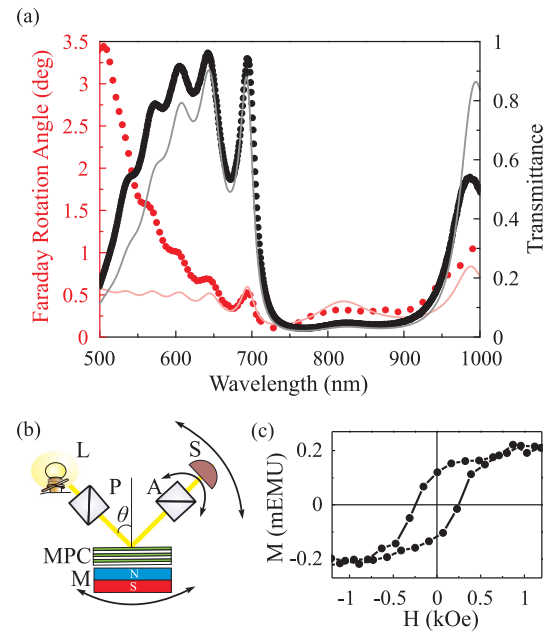


FIG. 3. (a) Spectra of transmittance (black) and Faraday rotation angle (red) of the MPC sample measured (dots) and calculated (curves) for the normal incidence. (b) Sketch of the experiment. (c) Hysteresis loop of the sample.

light through the layered structure and low group velocity of light near the photonic band gap edge. The growth of the Faraday angle in the short-wave part of the spectrum caused by the increase in gyration vector values due to the dispersion of Bi:YIG was not taken into account in the numerical model. The calculation results are in a good agreement with the experimental data for the wavelengths above 650 nm that confirms the correct choice of the model parameters in the studying spectral range.

BSW and WGM having dispersion curves located behind the light line require prism- or lattice-coupling schemes to be excited. Here, we used the reflective Kretschmann configuration based on an isosceles BK7-glass prism with a base angle of 55°, which was set in place of the sample in the setup shown in Fig. 3(b). Figure 4 presents the measured and calculated s - (blue curves) and p -polarized (red curves) reflectance spectra of the magnetophotonic crystal and the corresponding spectra of the Faraday rotation (black curves) measured for s -polarized incident light. The angle of incidence from the prism to the sample surface, θ , varies from 42.6° (top panel) to 46.5° (bottom panel). As expected, the incidence of the s -polarized light results in the BSW excitation, which corresponds to a narrow shallow resonance in the reflectance spectra. The resonance depth decreases as the incident angle increases. This is caused by the decrease in the total amount of light energy penetrating into the MPC, while the incident angle increases behind the light line even though the field localization in the BSW increases. Wide dips in the red curves correspond to the WGM resonances while the magnetophotonic crystal is illuminated by p -polarized light. As the incident angle increases, both the resonances shift to short wavelengths, but the WGM resonance shifts faster; thus, the spectral distance between the BSW and WGM

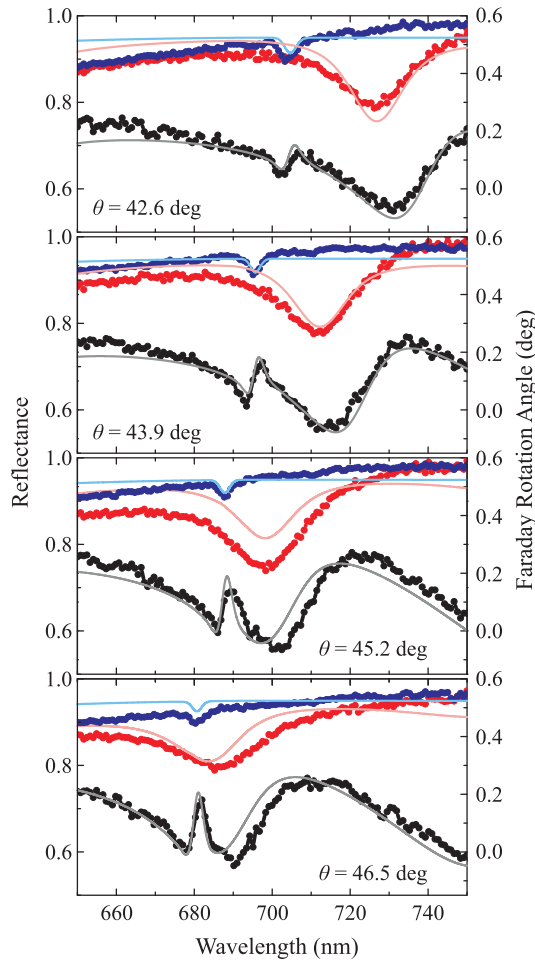


FIG. 4. Measured (dots) and calculated (curves) spectra of the Faraday rotation angle (black) and reflectance (blue) of s -polarized light. Measured (dots) and calculated (lines) spectra of reflectance (red) of p -polarized light are shown for reference. Angles of incidence at the sample from the prism are 42.6° , 43.9° , 45.2° , and 46.5° .

resonances decreases. The spectral dependence of the Faraday rotation angle of s -polarized light has a feature coinciding in wavelength and caused by the BSW excitation. The process is quite similar to Faraday rotation enhancement by the optical Tamm states in magnetophotonic crystals [2]. The BSW is an allowed state inside the photonic band gap that has a long lifetime and strong spatial localization of the electromagnetic field. The maximum of the field is reached inside the top layer of the magnetophotonic crystal [Fig. 2(b)], which is a magnetic one. Moreover, the resonance of the BSW is extremely narrow. All three of these factors contribute to the enhancement of the Faraday rotation. Surprisingly, the experimentally obtained value of the Faraday rotation angle is not large and reaches 0.2° . We believe that the angular divergence of the incident beam and sample surface roughness have decreased the observed value. The angular divergence of the incident beam of 20 mrad was taken into account during the calculations, providing a good agreement between the calculated and experimental data. The feature in the Faraday rotation spectrum has a Fano resonance shape and changes from an asymmetric shape to a symmetric one, while

the incident angle increases and the BSW and the WGM resonances approach each other. This behavior is observed both in the experiment and calculations. Thus, it can be argued that the spectral dependence of the Faraday rotation angle depends not only on the BSW resonance in the structure but also on the coupling of the BSW with the WGM mode that is not excited in the s polarization of the incident light. A certain analogy can be drawn here with the bright and dark modes of surface plasmons in plasmonic nanostructures [25]. Although the dark mode is not excited in the given experimental geometry, the Fano-shaped resonance in the Faraday rotation spectra enables visualization of the dark mode through the interaction with the bright mode. Moreover, the view of the resonance provides a means for determining the mutual spectral position of the BSW and WGM resonances.

A more general idea of the polarization changes produced by the magnetophotonic crystal undergoing an external magnetic field action can be given by a study of the spectral dependences of the Stokes parameters (e.g., see Ref. [26]) of reflected light. The parameter S_0 corresponds to the reflectance; the Faraday angle φ is related to the first and second Stokes parameters as $\varphi = (1/2) \arctan(S_2/S_1)$. The Stokes parameter S_3 describes the ellipticity introduced by a magnetophotonic crystal, which also increases significantly if the Faraday rotation angles are large. Figure 5 shows three typical cases: when the WGM resonance is blueshifted for 30 nm [Fig. 5(a)], redshifted for 30 nm [Fig. 5(c)] relative to the BSW resonance, and when they coincide [Fig. 5(b)]. The results are obtained by changing the thickness of the top layer at the magnetophotonic crystal/air interface and calculated for top layer thicknesses of 390 nm, 428 nm, and 470 nm at an angle of incidence of $\theta = 42.6^\circ$. The top layer thickness of 390 nm corresponds to the sample structure studied experimentally.

Let us consider the reflection of the sample with the top-layer thickness of 428 nm [Fig. 5(b)]. The spectrum of S_0 demonstrates the deepest minimum of the reflectance. This is not directly related to the BSW and WGM spectral positions. This indicates that the BSW excitation conditions in the structure are optimal and the BSW coupling is most effective. It allows one to demonstrate most clearly the possibilities of the BSW application for magnetically controlled light polarization transformations. The S_1/S_0 and S_2/S_0 spectra show that the more effective BSW is excited in the structure, the greater Faraday rotation can be achieved. Bandwidth of the BSW resonance is extremely small, and spectral dependence of phase of light reflected from the MPC is steplike and has a jump across the BSW resonance spectral position [19]. The magnetoinduced splitting of the resonance [15] leads to phase difference between left and right circularly polarized waves that is much larger than values determined by magneto-optical constants of magnetic layers. Under ideal conditions the Faraday rotation can reach a theoretical limit of $\pi/2$. At the same time, the ellipticity of light reflected from the structure increases (Fig. 5, S_3/S_0 spectrum) because of different dispersion relations of TE and TM modes of the MPC. Near the BSW resonance the ellipticity reaches 1, that corresponds to circularly polarized light. With a decrease of the efficiency of the BSW coupling, the magnitudes of the Stokes

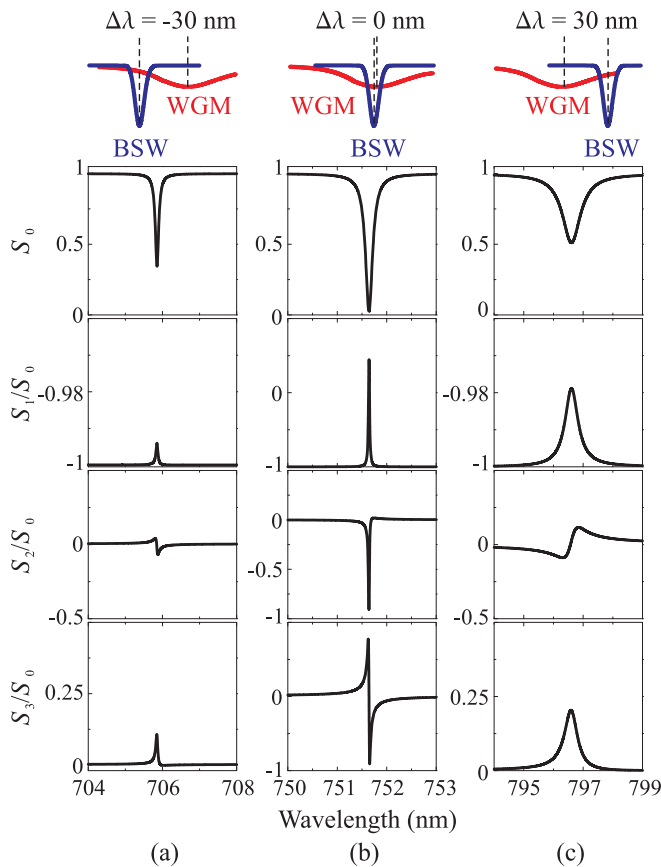


FIG. 5. Numerical spectra of the Stokes parameter S_0 and normalized Stokes parameters S_1/S_0 , S_2/S_0 , S_3/S_0 of light reflected by the magnetophotonic crystals in the presence of magnetic field. The incident light is s -polarized plane wave. The thicknesses of the top layer at the magnetophotonic crystal/air interface are 390 nm (a), 428 nm (b), and 470 nm (c). $\theta = 42.6^\circ$.

parameters spectral resonances drastically decrease [Figs. 5(a) and 5(c)]. Thus, the considering MPC structure near the BSW

resonance is a magnetically-controlled wave plate of variable thickness that can be of great potential for applications.

The influence of the WGM and its spectral position relative to the BSW manifests itself in the S_2/S_0 parameter spectral behavior. In the case where the BSW resonance wavelength is sufficiently shorter than one of the WGM resonance, the features in the S_2/S_0 spectrum and, correspondingly, in the Faraday rotation spectrum have an asymmetric form of the Fano resonance [Fig. 5(a)]. Then, the shape of the Fano resonance becomes symmetrical and appears as a dip, while the BSW and WGM resonances become closer and coincide [Fig. 5(b)]. When the BSW resonance shifts to a longer wavelength relative to the WGM, the Fano resonance in the S_2/S_0 spectrum takes an inverted asymmetrical shape [Fig. 5(c)]. This leads to the sign change of the Faraday rotation angle if the BSW dispersion curve crosses the WGM curve. Thus, the shape of the Fano resonance in the Faraday rotation angle spectrum is determined by the spectral positions of the BSW and WGM resonances relative to each other.

In conclusion, we have experimentally and numerically studied the behavior of the spectral dependence of the Faraday rotation angle in one-dimensional magnetophotonic crystals in the spectral vicinity of the BSW and WGM resonances existing for the orthogonal linear polarization of the incident light. In the case of closeness of the two resonances, a Fano-shaped feature appears in the Faraday rotation spectrum caused by the coupling of two modes, one of which is bright for a given polarization and the other one is a dark one. The Fano-shaped resonance in the spectrum of the Faraday polarization rotation angle reveals the presence of the dark mode and provides definite information about the relative positions of the resonances. Besides, it leads to the change of the Faraday rotation direction that makes these resonance MPCs promising for the future photonics devices.

This work was partially supported by the Russian Ministry of Education and Science (Grant No. 14.W03.31.0008), the Russian Foundation for Basic Research, and the Russian Science Foundation (Grant No. 15-12-00065, numerical simulations).

- [1] M. Inoue and T. Fujii, *J. Appl. Phys.* **81**, 5659 (1997).
- [2] T. Goto, A. V. Dorofeenko, A. M. Merzlikin, A. V. Baryshev, A. P. Vinogradov, M. Inoue, A. A. Lisiansky, and A. B. Granovsky, *Phys. Rev. Lett.* **101**, 113902 (2008).
- [3] A. A. Grunin, A. G. Zhdanov, A. A. Ezhov, E. A. Ganshina, and A. A. Fedyanin, *Appl. Phys. Lett.* **97**, 261908 (2010).
- [4] C. Clavero, K. Yang, J. R. Skuza, and R. A. Lukaszew, *Opt. Express* **18**, 7743 (2010).
- [5] J. Y. Chin, T. Steinle, T. Wehler, D. Dregely, T. Weiss, V. I. Belotelov, B. Stritzker, and H. Giessen, *Nat. Commun.* **4**, 1599 (2013).
- [6] M. Inoue, R. Fujikawa, A. Baryshev, A. Khanikaev, P. B. Lim, H. Uchida, O. Aktsipetrov, A. Fedyanin, T. Murzina, and A. Granovsky, *J. Phys. D* **39**, R151 (2006).
- [7] A. G. Zhdanov, A. A. Fedyanin, O. A. Aktsipetrov, D. Kobayashi, H. Uchida, and M. Inoue, *J. Magn. Magn. Mater.* **300**, e253 (2006).
- [8] A. B. Khanikaev, A. B. Baryshev, P. B. Lim, H. Uchida, M. Inoue, A. G. Zhdanov, A. A. Fedyanin, A. I. Maydykovskiy, and O. A. Aktsipetrov, *Phys. Rev. B* **78**, 193102 (2008).
- [9] S. Murai, S. Yao, T. Nakamura, T. Kawamoto, K. Fujita, K. Yano, and K. Tanaka, *Appl. Phys. Lett.* **101**, 151121 (2012).
- [10] A. I. Musorin, M. I. Sharipova, T. V. Dolgova, M. Inoue, and A. A. Fedyanin, *Phys. Rev. Appl.* **6**, 024012 (2016).
- [11] E. Takeda, N. Todoroki, Y. Kitamoto, M. Abe, M. Inoue, T. Fujii, and K. Arai, *J. Appl. Phys.* **87**, 6782 (2000).
- [12] S. Kahl and A. M. Grishin, *Appl. Phys. Lett.* **84**, 1438 (2004).
- [13] S. I. Khartsev and A. M. Grishin, *J. Appl. Phys.* **101**, 053906 (2007).
- [14] T. Goto, A. V. Baryshev, K. Tobinaga, and M. Inoue, *J. Appl. Phys.* **107**, 09A946 (2010).
- [15] M. J. Steel, M. Levy, and R. M. Osgood, *J. Lightwave Technol.* **18**, 1297 (2000).
- [16] P. Yeh, A. Yariv, and A. Y. Cho, *Appl. Phys. Lett.* **32**, 104 (1978).

- [17] W. M. Robertson and M. S. May, *Appl. Phys. Lett.* **74**, 1800 (1999).
- [18] E. Descrovi, T. Sfez, M. Quaglio, D. Brunazzo, L. Dominici, F. Michelotti, H. P. Herzig, O. J. F. Martin, and F. Giorgis, *Nano Lett.* **10**, 2087 (2010).
- [19] I. V. Soboleva, V. V. Moskalenko, and A. A. Fedyanin, *Phys. Rev. Lett.* **108**, 123901 (2012).
- [20] E. Guillermain, V. Lysenko, and T. Benyattou, *J. Lumin.* **121**, 319 (2006).
- [21] M. N. Romodina, I. V. Soboleva, and A. A. Fedyanin, *J. Magn. Mater.* **415**, 82 (2016).
- [22] D. W. Berreman, *J. Opt. Soc. Am.* **62**, 502 (1972).
- [23] D. S. Bethune, *J. Opt. Soc. Am. B* **8**, 367 (1991).
- [24] I. V. Soboleva, M. N. Romodina, K. A. Korzun, A. I. Musorin, and A. A. Fedyanin, *Proc. SPIE* **10112**, 1011210 (2017).
- [25] C. Ropers, D. J. Park, G. Stibenz, G. Steinmeyer, J. Kim, D. S. Kim, and C. Lienau, *Phys. Rev. Lett.* **94**, 113901 (2005).
- [26] W. A. Shurcliff, *Polarized Light. Production and Use* (Harvard University Press, Cambridge, MA, 1962).